ACS OMEGA

http://pubs.acs.org/journal/acsodf

Article

# HACC-Based Nanoscale Delivery of the NbMLP28 Plasmid as a Crop Protection Strategy for Viral Diseases

Daoshun Zhang,[#] Liyun Song,[#] Zhonglong Lin, Kun Huang, Chunming Liu, Yong Wang, Dongyang Liu, Songbai Zhang,* and Jinguang Yang*

Cite This: *ACS Omega* 2021, 6, 33953−33960

Read Online

ACCESS | Metrics & More | Article Recommendations

**ABSTRACT:** Resistant genes as an effective strategy to antivirus of plants are at the core of sustainability efforts. We use the antiviral protein major latex protein 28 (NbMLP28 plasmid) and *N*-2-hydroxypropyl trimethyl ammonium chloride chitosan (HACC) designated as the HACC/NbMLP28 complex as protective gene delivery vectors to prepare nanonucleic acid drugs. The maximum drug loading capacity of HACC was 4. The particle size of HACC/NbMLP28 was measured by transmission electron microscopy and found to be approximately 40−120 nm, the particle dispersion index (PDI) was 0.448, and the $\zeta$-potential was 22.3 mV. This facilitates its ability to deliver particles. Different controls of laser scanning confocal experiments verified the effective expression of NbMLP28 and the feasibility of nanodelivery. The optimal ratio of HACC/plasmid was 2:1. Finally, the nanoparticle/plasmid complex was tested for its ability to control diseases and was found to significantly improve resistance to three viruses. The enhanced resistance was particularly notable 4 days after inoculation. Taken together, these results indicate that HACC/NbMLP28 is a promising tool to treat plant viruses. To the best of our knowledge, this is the first study that successfully delivered and expressed antiviral protein particles in plants. This gene delivery system can effectively load antiviral plasmids and express them in plant leaves, significantly affecting the plant resistance of three RNA viruses.

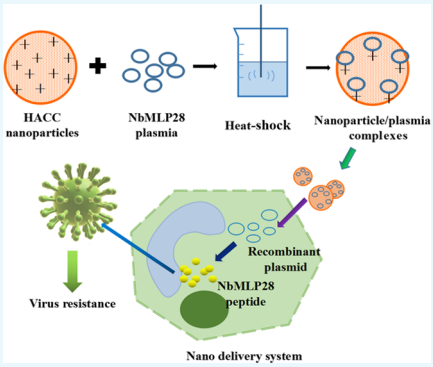


## INTRODUCTION

Plant viral diseases are widely distributed, pose a serious threat to agriculture and forestry production, and cause enormous economic losses of more than 50 billion euros per year worldwide,[1] making them the main factors that affect the yield and quality of crops.[2] Tobacco mosaic virus (TMV), cucumber mosaic virus (CMV), and potato virus Y (PVY) are among the top five viruses that harm plants.[3] The current measures to control plant viral disease rely heavily on aphid prevention, agronomic practices, and virus-resistant plant varieties. The effectiveness of these control methods is not clear, and the use of transgenic technology and pesticides causes major problems such as environmental pollution due to pesticide residues. Therefore, the use of biotechnology to promote the cure of plant diseases, particularly the effective control of plant viral diseases, remains an urgent problem.

As an abundant laticifer-specific peptide, the major latex protein NbMLP28 was first identified from the latex of opium poppy (*Papaver somniferum*).[4] NbMLP28 proteins are members of the NbMLP28 subfamily of the Betv1 family and exist in many plant species. The orthologues of NbMLP28, the NbMLP28-like proteins, are also found in various plant species, including *Arabidopsis thaliana*, soybean, and tobacco. Previous studies in our laboratory have found that transgenic plants overexpressing NbMLP28 have significantly enhanced resistance to viruses.[5] We have also observed an enhanced virus resistance at both the mRNA and protein levels in *N. benthamiana* overexpressing NbMLP28. The transformants primarily express an antiviral effect compared with the control group. However, the use of this vector is susceptible to host-specific limitations and can only be used in some species of plants.[6] Therefore, we sought to use the plasmid constructed with the NbMLP28 gene that harbors the 35S promoter to complete a plant antiviral experiment based on the new delivery strategy of nanomaterials.

Gene therapy has become a frontier area of research, particularly with advances in nanotechnology.[7] Delivery is a critical challenge in plants since common abiotic transfection techniques, such as heat shock, electroporation, and lipid- and polymer-mediated delivery, that are used for microbes and animals are typically ineffective in intact plants.[8] In addition,

**Received:** September 23, 2021
**Accepted:** November 15, 2021
**Published:** November 29, 2021

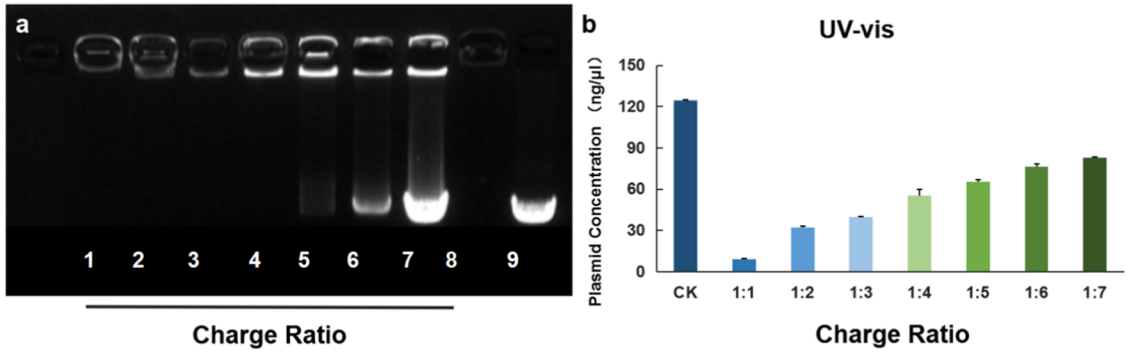


**Figure 1.** Agarose gel retention results of DNase I protection assay. (a) Lane 1: nanoparticle/plasmid complex (HACC/NbMLP28 plasmid 1:1); lane 2: nanoparticle/plasmid complex (HACC/NbMLP28 plasmid 1:2); lane 3: nanoparticle/plasmid complex (HACC/NbMLP28 plasmid 1:3); lane 4: nanoparticle/plasmid complex (HACC/NbMLP28 plasmid 1:4); lane 5: nanoparticle/plasmid complex (HACC/NbMLP28 plasmid 1:5); lane 6: nanoparticle/plasmid complex (HACC/NbMLP28 plasmid 1:6); lane 7: nanoparticle/plasmid complex (HACC/NbMLP28 plasmid 1:7); lane 8: bare nanomaterials used as CK negative controls (HACC); and lane 9: naked plasmid was used as the CK positive control. (b) Plasmid concentration of the supernatant under different charge ratios of nanoparticle/plasmid complex.

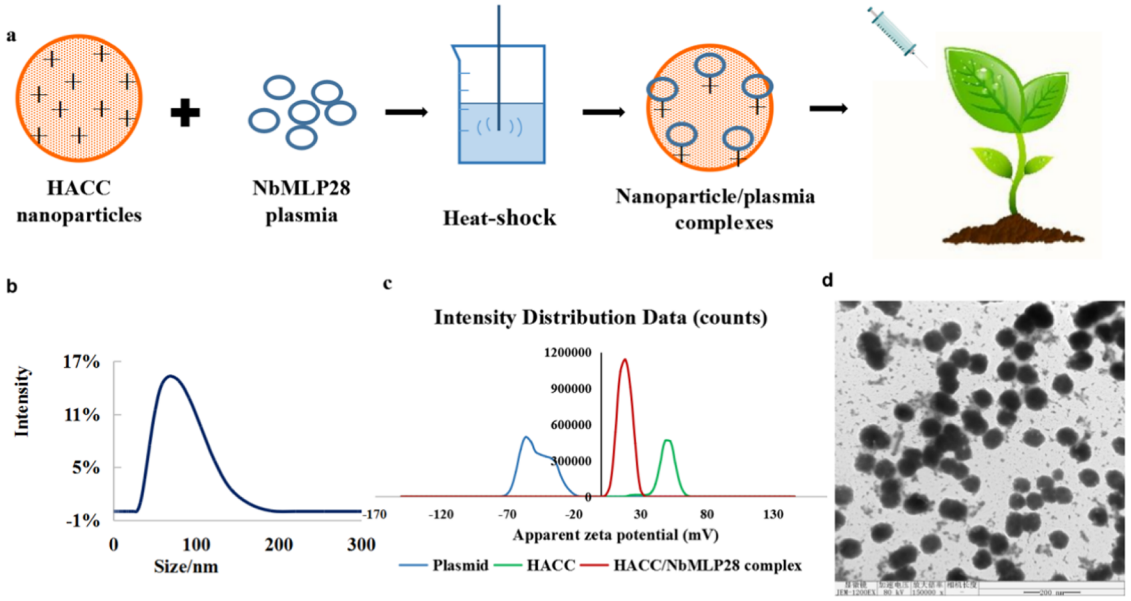


**Figure 2.** Characterization of the HACC/NbMLP28 complex. (a) The HACC/NbMLP28 complex was prepared by HACC nanoparticles mimic-loaded NbMLP28 plasmid using the heat-shock method and injected into plants. (b) Nanometer particle size. (c) Nanometer $\zeta$-potential of pure plasmids nanomaterial of HACC and HACC/NbMLP28 complex prepared at an N/P ratio of 2:1. (d) Transmission electron microscopy (TEM) image of the HACC/NbMLP28 complex prepared at an N/P ratio of 2:1 and accelerated voltage of 80 kV at 150 000 magnification.

the plant gene delivery tools, such as *Agrobacterium*-mediated transformation, that have been used traditionally either limit the range of plant species that can be transformed or exhibit low transformation efficiencies and tissue damage from the use of a high external force.[9] Therefore, the focus of this research is to use a simple method to transport corrective nucleic acids into specific cells as molecular treatments to inhibit or interfere with some deleterious or foreign genes *in vivo*. In short, the combination of plasmid DNA and nanomaterials can efficiently encode the transient expression of proteins and have a protective effect on the degradation of nucleases in plants. The key challenge in successful gene therapy is the development of safe and efficient delivery vehicles and methods.[10] The preparation of *N*-2-hydroxypropyl trimethyl ammonium chloride chitosan (HACC) by the chemical modification of the quaternary ammonium salt group of chitosan can solve the problems of poor stability, difficult dissociation, and a low transfection rate of the HACC–NbMLP28 nanocomplex under neutral conditions.[11] Compared with other nanomaterials, HACC is inexpensive, biocompatible, typically not cytotoxic,[12] effective in controlling the drug release rate,[13] and high polycation with a positive charge.[14] Also, it easily combines with nucleic acids owing to their negative charges. In this study, we demonstrated the delivery and ability of the nanocomplex to express proteins and the separate resistance of the HACC/NbMLP28 nanocomplex to three types of viruses. To the best of our knowledge, this is the first study that successfully delivered and expressed antiviral protein particles in plants. This gene delivery system plays a key role in the scale-up and economics production of plants with broad-spectrum viral resistance.

## RESULTS

**Optimal Drug Loading of the HACC/NbMLP28 Complex.** To detect the binding of nanoparticles to plasmids, we used a gel retardation assay to detect different N/P ratios


https://doi.org/10.1021/acsomega.1c05295
ACS Omega 2021, 6, 33953−33960

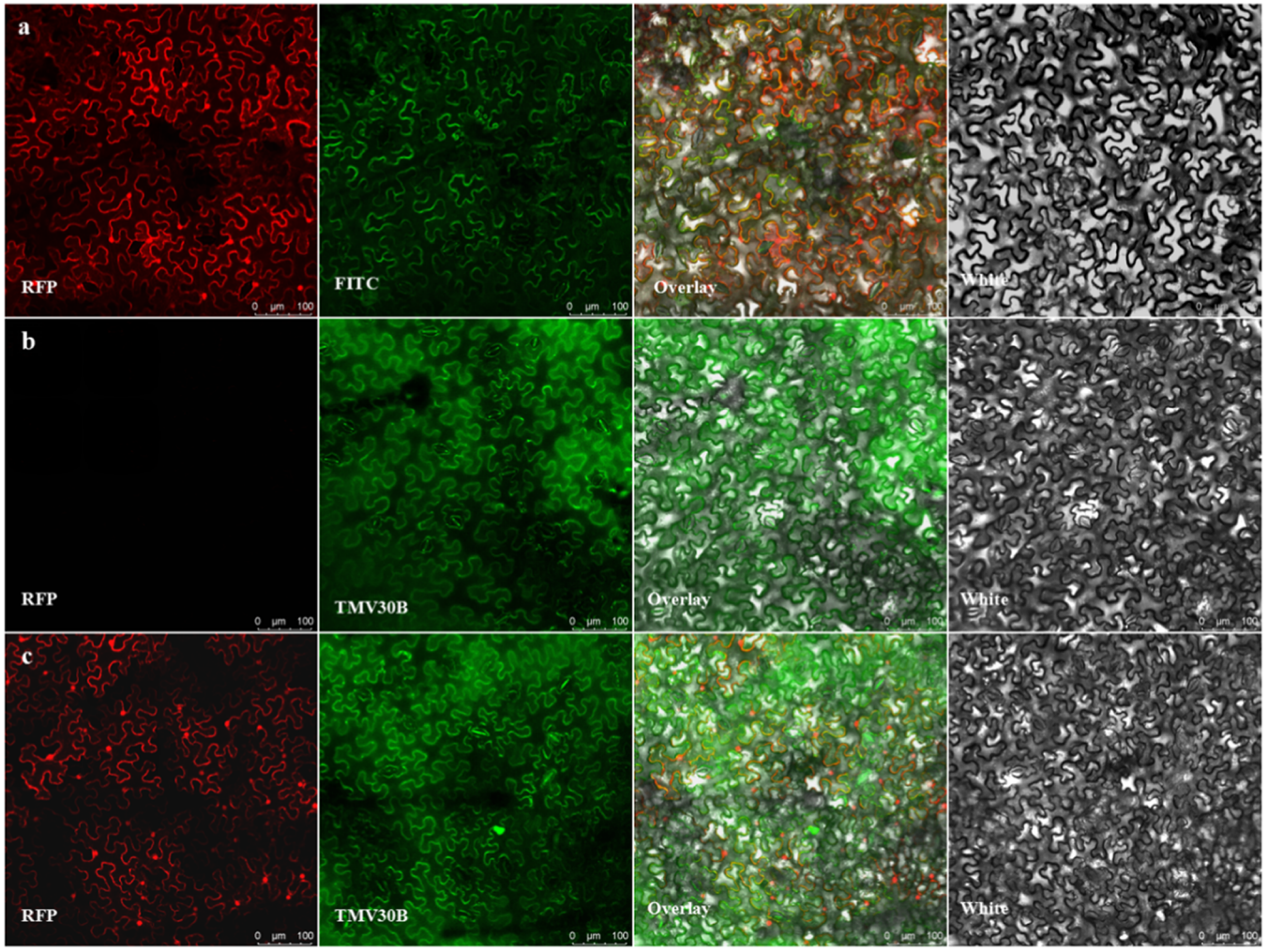


**Figure 3.** Expression and nanodelivery results of HACC/NbMLP28 *in vivo*. (a) *N. benthamiana* leaves infiltrated with the NbMLP28/HACC complex are imaged with confocal microscopy to determine the levels of RFP expression and the deliverability of HACC in the leaf lamina of each plant. Among them, the NbMLP28 plasmid harbored the GFP fluorescence gene, and the nanomaterial HACC was labeled by FITC. (b) *N. benthamiana* leaves infiltrated with TMV30B-HACC/NbMLP28. (c) *N. benthamiana* leaves infiltrated with TMV30B-NbMLP28. FITC, fluorescent isothiocyanate; GFP, green fluorescent protein; RFP, red fluorescent protein.

(the ratio of moles of the amine groups of polyethylene imine (PEI) to moles of the phosphate groups of plasmids). The evaluation of the intensity of the agarose gel band is recommended to get a quantitative idea of how much plasmids interact with nanoparticles. Representative bands from gel electrophoresis are shown when the N/P ratio is 1:5. This indicates that HACC can be fully coated with the NbMLP2828 plasmid when the N/P ratio is 1:4. The results indicate that the complexation of the nanoparticles and plasmids in an N/P ratio of 1:4 shows excellent retardation, with the drug loading capacity of HACC of 4 (Figure 1). The plasmid concentration of the supernatant was positively correlated with different charge ratios of HACC/NbMLP28 complexes, proving that the drug loading capacity of HACC to plasmids correlated with the N/P ratio (Figure 2).

**Characterization of the HACC/NbMLP28 Complex.** To prepare the gene delivery system, we first loaded plasmids onto nanoparticles to form nanoparticle/plasmid complexes and then determined the nanocharacterization of the HACC/NbMLP2828 complexes. The diameters of these complexes were determined further by dynamic light scattering (DLS), and the average diameter of the complexes was 65 nm and the particle dispersion index (PDI) of the complexes was 0.407 (Figure 2b). The pure chitosan quaternary ammonium salt had an average particle size of 1730 nm and a particle dispersion index (PDI) of 0.448. The $\zeta$-potential value of the nanoparticle/plasmid complexes was examined in more detail using a potential measurement analyzer. The $\zeta$-potential values of plasmids, nanomaterials, and their complexes with an N/P ratio of 2:1 were approximately −54.6, 50.7, and 22.3 mV, respectively (Figure 2c). These results showed that the surface of the HACC/NbMLP28 complex was positively charged, and the mass of HACC was relatively higher than that of the plasmid. This was consistent with the estimated value. The plasmid was fully encapsulated, which facilitates the complete delivery of nanodrugs. The morphology of nanoparticle/plasmid complexes was examined by transmission electron microscopy (TEM), which indicated that the HACC/NbMLP2828 complexes were spherical (Figure 2d).

**Transient Expression and Localization Analysis of HACC/NbMLP28 *In Vivo*.** The expression of the NbMLP28 plasmid was detected using laser scanning confocal microscopy (LSCM). Seventy-two hours after infection, the HACC/NbMLP28 complex had strong fluorescence on the cytoplasm.


https://doi.org/10.1021/acsomega.1c05295
*ACS Omega* 2021, 6, 33953−33960

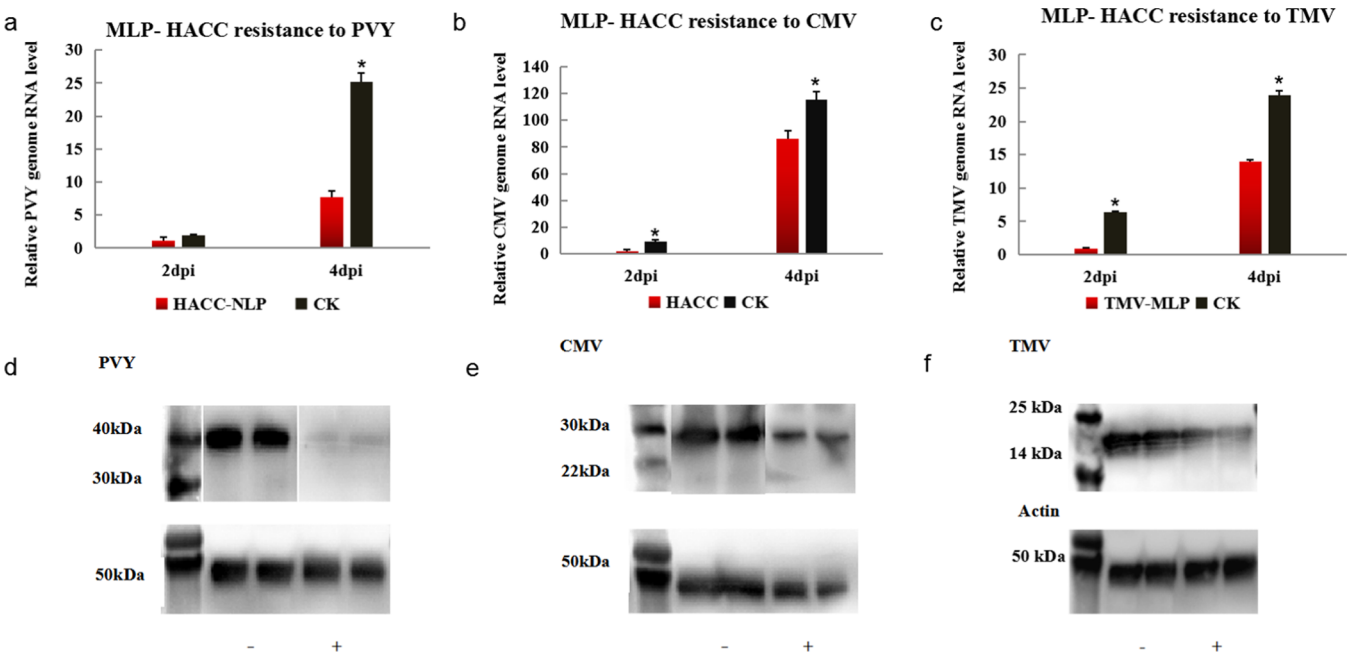


**Figure 4.** qRT-PCR and Western blot were used to detect the expression of the viruses. (a) qRT-PCR analysis of the levels of expression of PVY cDNA on days 2 and 4 in HACC/NbMLP28-treated *N. benthamiana* leaves. (b) qRT-PCR analysis of the levels of expression of CMV cDNA on days 2 and 4 in *N. benthamiana* (tobacco) leaves treated with HACC/NbMLP28. (c) qRT-PCR analysis of the levels of expression of TMV cDNA on days 2 and 4 in *N. benthamiana* leaves treated with HACC/NbMLP28. (d) Western blot analysis with the PVY CP antibody. (e) Western blot analysis with the CMV CP antibody. An antibody to $\beta$-actin was used as the loading control. (f) Western blot analysis with the TMV CP antibody. $\beta$-Actin antibody was used as a loading control. Tobacco leaves inoculated with HACC/NbMLP28 were used as the mock treatment. Negative NbMLP28 was the control group, and positive NbMLP28 was the treatment group. There were two biological replicates. CMV, cucumber mosaic virus; Dpi, day past inoculation; PVY, potato virus Y; qRT-PCR, quantitative real-time reverse transcriptase PCR; TMV, tobacco mosaic virus. Data represent the average of at least three experiments, with the error bars representing the standard error of the mean ($n = 3$). The data were analyzed with an independent sample *T*-test using IBM SPSS Statistics v.25 software, * indicated that values of the two treatments were significantly different at $P < 0.05$.

The red fluorescence came from RFP tags carried on the NbMLP28 plasmid and the green fluorescence came from the FITC-treated HACC (Figure 3a). The results showed that there was red fluorescence in the mesophyll cells of *N. benthamiana* 3 days later, and the NbMLP28 gene was expressed in the *N. benthamiana* leaves (Figure 3b). Laser confocal microscopy results revealed that the vector TMV30B-HACC/NbMLP28 fluoresced in the cell membrane and cytoplasm (Figure 3b). However, the negative control sample TMV30B-NbMLP28 had no visible red fluorescence (Figure 3c); these results indicate that the nanomaterial HACC plays a key role in gene delivery and plasmid expression.

The expression in plants was determined by RFP tags on the plasmid, and the ability of the nanomaterial delivery carrier was determined by the FITC labeling of chitosan quaternary ammonium salt. TMV30B carries GFP tags and detects the expression of the NbMLP28 gene under viral infection by its transient infection. Different treatment schemes were used to determine the efficacy of different complexes, and the HACC/NbMLP28 complex was established to have the best ratio to obtain the relatively highest expression.

**Antiviral Effect of HACC/NbMLP28.** To test the effect of the HACC/NbMLP28 complex resistance to viral infection, we inoculated TMV, PVY, or CMV into *N. benthamiana* after infiltration with the HACC/NbMLP28 complex. In addition, the levels of the viral coat protein (CP) gene and protein expression were measured using qRT-PCR and Western blotting, respectively.

The levels of gene expression of different treatments on days 2 and 4 were analyzed by quantitative real-time PCR. We observed that inoculation of the PVY virus at 4 dpi resulted in a 2 times higher level of expression of the PVY CP protein in the control group compared with that in the treatment group. The expression of the CP protein of the PVY control group was significantly different from that of the treatment group (Figure 4a). After inoculation with the TMV virus, the expression of the CP protein of the *N. benthamiana* control group was significantly different from that of the treatment group, and the difference was significant on day 4 (Figure 4c). After inoculation with the CMV virus, the expression of the CP protein in the *N. benthamiana* control group was significantly different from that of the treatment groups (Figure 4b). By contrast, at 4 dpi, the PVY expression was reduced by 69.6%, CMV expression by 25.5%, and TMV expression by 41.3%, and the treated plants showed the strongest resistance to the PVY virus. The virus was found to be highly expressed in the control group and significantly inhibited in the treatment group. This indicates that HACC/NbMLP28 had some broad-spectrum resistance to the three viruses.

The transfection efficiency and gene expression of the gene complexes were evaluated using a Western blot assay. To detect the expression of TMV, PVY, and CMV proteins in different experimental groups after inoculation with the viruses, we used Western blotting for the molecular analysis to evaluate the ability of the complex to interfere with the expression of viral proteins. The results showed that the level of protein expression in the control group was significantly higher than


https://doi.org/10.1021/acsomega.1c05295
*ACS Omega* 2021, 6, 33953−33960

that in the treatment group, and the protein bands were in the corresponding positions (Figure 4d–f). These results provide further evidence that the HACC/NbMLP28 complex can effectively transfer target genes to *N. benthamiana* leaves, and the HACC/NbMLP28 nanoparticle/plasmid complex can be effectively expressed in plants and strongly inhibit viral expression.

Visually, the shape of *N. benthamiana* leaves in the control group (empty plasmids and HACC) was significantly different from those in the treatment group (HACC/NbMLP28) 6 days after inoculation with CMV, PVY, and TMV, respectively. The *N. benthamiana* leaves in the control group exhibited more obvious necrosis, wrinkling, and uneven thickness (Figure 5). This verifies the feasibility of using this gene delivery system to express relevant proteins in plants for antiviral experiments.

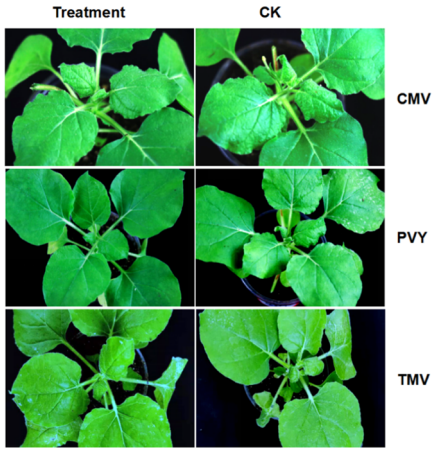


**Figure 5.** Characterization of *N. benthamiana* leaves. The shape of *N. benthamiana* leaves in the control group (CK-HACC/empty plasmid) was significantly different from those of the treatment group (HACC/NbMLP28) 6 days after inoculation with CMV, PVY, and TMV. The leaves in the control group had more obvious necrosis, wrinkling, and uneven thickness. All of the experiments were conducted with intact leaves that were attached to healthy plants. CMV, cucumber mosaic virus; PVY, potato virus Y; TMV, tobacco mosaic virus.

In this study, we demonstrated the separate resistance of the HACC/NbMLP28 nanocomplex formed by encapsulating pDNA/nanomaterials together with three viruses. The ability of the recombinant plasmid to control viruses in tobacco leaves was analyzed by the difference in the levels of expression of the viruses.

## MATERIALS AND METHODS

**Sample Preparation.** The experimental plant was tobacco (*N. benthamiana*). The infectious clone TMV30B was obtained from the Virus Research Group of the Tobacco Research Institute, Chinese Academy of Agricultural Sciences (Qingdao, China). For inoculation, TMV30B-GFP was obtained from the Key Laboratory of Tobacco Pest Monitoring (Qingdao, China). *N. benthamiana* was grown in a greenhouse with a photoperiod of 16/8 h (light/dark) at 25 °C. The leaves of two replicates were collected from 4-week-old tobacco seedlings for downstream experiments. The Qin[15] method was used to prepare the solutions of TMV, PVY, and CMV. The leaves of *N. benthamiana* seedlings were inoculated with solutions of TMV, PVY, and CMV by rubbing. Rubbing caused mechanical damage to the leaves after spraying quartz sand evenly on the leaves, thereby the virus effectively infected the plants. Tobacco leaves were collected at 2 and 4 days after inoculation (dpi). Three biological replicates were assessed.

**Preparation of HACC Nanoparticles.** Two grams of HACC powder was dissolved in 100 mL of pure water that had been sterilized in an autoclave. The resulting mixture was stirred magnetically at room temperature to obtain 0.2 mg/mL HACC. An aqueous solution of HACC (μg/mL, mg/mL) was prepared based on the concentration of plasmid and adjusted to concentrations of 2-, 5-, and 10-fold of plasmid DNA. The plasmid was added to an aqueous solution of HACC drop by drop at room temperature and then magnetically stirred at 400 rpm for 10 min. The solution was incubated at 55 °C for 1 min, vibrated for 30 s, and then incubated at room temperature for 10 min to obtain the mixed solution.

**Preparation of Expression Vectors.** A Gate100 vector was constructed and NbMLP28 was then inserted into the pEarlyGate100 expression vector of carrier GFP tags that contains the 35S promoter. The NbMLP28 plasmids were then sequenced to confirm that the NbMLP28 genes were inserted correctly. Since the NbMLP28 vector contains the NbMLP28 gene, it can be used to detect the efficiency of transfection in tissues or cultures. RFP tags were inserted into the constructed vector for subsequent gene expression verification. The constructed vector was transformed into an *Escherichia coli* strain, and the bacterial liquid was identified by PCR. The plasmids were extracted using a Fast Pure Endo Free Plasmid Maxi Kit (DC202-01; Vazyme, Nanjing, China). The measured concentration of plasmid was between 200 and 1200 ng/μL, the average optical density (OD) A260/A280 was 1.89, and the purity of plasmid was up to the grade of the QA/QC standard. The plasmid was amplified by PCR with a GATE100 primer and suitable bands were detected by agarose gel electrophoresis and stored at −20 °C.

**Preparation of Nanoparticle/Plasmid Complexes.** The quaternary ammonium salt of chitosan nanoparticles was used as the delivery carrier of pDNA and assembled by the electrostatic force between the positive amino charge in the quaternary ammonium salt of chitosan and the negative charge on the nucleotide of the plasmid. The quaternary ammonium salt of chitosan was coated with the plasmid to form spherical nanoparticles. *N*-2-Hydroxypropyl trimethyl ammonium chloride chitosan solvent was dissolved in sterile water and stirred in a magnetic mixer for 6 h to obtain a solution of HACC at a concentration of 200 ng/μL.

The plasmid was diluted in 100 μL of sodium sulfate (20 mM) and added to 100 μL of HACC solution drop by drop. The mixture was heated at 55 °C for 1 min, immediately swirled at high speed for 30 s, and incubated at room temperature for 1 h to promote the formation of nanoparticles. The nanoparticle/plasmid complex (HACC/NbMLP28) was formed for subsequent detection.

**Drug Loading and Characterization.** The interaction between plasmids and nanoparticles under different ratios of N/P was detected by a gel retardation assay. To test the ability of nanoparticles to bind plasmids, a gel mobility shift assay was used to detect different ratios of N/P (the molar ratio of the amine group of polyethylene imine (PEI) to the phosphate group of the plasmid), which represent the ratio of the weight between the directly used and the NbMLP28/pDNA complex. We used seven ratios of N/P (10:1, 2:1, 1:1, 1:2, 1:5, 1:10, and 1:20) as the control group for the antiviral reagent, and pure


https://doi.org/10.1021/acsomega.1c05295
ACS Omega 2021, 6, 33953−33960

plasmids and pure HACC liquid of the same mass as the positive and negative controls, respectively.

The samples of the recombinant plasmid (10 $\mu$L), various HACC/recombinant plasmid nanoparticles (10 $\mu$L), and pure solutions of HACC (10 $\mu$L) were mixed with 2 $\mu$L of the gel loading buffer. The gel was stained with Gel Red and loaded onto a 1.0% agarose gel in TBE buffer at pH 8.0. The samples were electrophoresed at 80 V for 30 min and visualized under UV light. Then, we used a UV spectrophotometer to measure the plasmid concentration of the supernatant of the nanomaterial plasmid complex under different charge ratios.

**Characterization of the HACC/NbMLP28 Complex.** The potential of nanoparticle/plasmid complexes was determined by a potential measurement (Zetasizer Nano ZS90, U.K.) analyzer as the average of the three experiments. The nanomaterial plasmid complex was dropped onto a copper film with a carbon mesh, dried, and observed under a vacuum electron microscope. In brief, the morphology of nanoparticle/plasmid complexes was observed by scanning electron microscopy (SEM) and a Nanometer particle size potential analyzer (Malvern Nano ZS90, U.K.). The scanning image, particle size, and $\zeta$-potential of the composite were obtained.

**Expression and Localization Were Measured by Laser Scanning Confocal Microscopy.** The preparation of HACC/NbMLP28/RFP was used to determine whether the target protein NbMLP28 was expressed in the leaves of *N. benthamiana*. We used HACC with a fluorescein isothiocyanate (FITC) label to encapsulate the NbMLP28 plasmid with an RFP label. To detect the efficiency of the expression of the HACC/NbMLP28 complex and the delivery effect of nanomaterials, a TMV30/GFP vector was transformed into *Agrobacterium tumefaciens* and then instantaneously used to infect tobacco. The HACC/NbMLP28-RFP complex and NbMLP28-RFP pure plasmid were injected, respectively. Laser scanning confocal microscopy was used to measure the expression of the NbMLP28 plasmid in the leaves of *N. benthamiana*. A 0.5 $cm^2$ section of an inoculated leaf was placed on a slide and observed under a confocal laser microscope. The NbMLP28 plasmids were labeled with RFP tags, and red fluorescence could be observed under a confocal microscope. TMV30B was tagged with the gene for green fluorescent protein (GFP), and green fluorescence could be observed under a confocal laser microscope after the instantaneous infection of *N. benthamiana* leaves.

HACC was labeled with FITC, which was dissolved in DMSO at a concentration of 1 mg/mL, and a 1% solution of *N*-2-hydroxypropyl trimethyl ammonium chloride chitosan solution was prepared with water. An equal volume of FITC was mixed with a solution of *N*-2-hydroxypropyl trimethyl ammonium chloride chitosan, stirred at room temperature for 3 h in the dark, and dialyzed at 8000−14 000 Da for 3 days to obtain HACC/FITC. FITC should fluoresce green under a confocal laser microscope.

The sample of HACC/NbMLP28/RFP uses mCherry fluorescent in 552 nm as an excitation light with an intensity of 8.78 and a receiving light of 506−533. The mCherry and TIFC wavelengths of the samples of HACC/NbMLP28/TMV30B and HACC/NbMLP28/FITC were 488 nm as the excitation light, and the light intensity was 5.75 and the received light was 603−643. QA/QC procedures were strictly followed during method implementation.

**qPT-PCR Assay.** The empty carrier and HACC were used as control groups. When the experimental plant was grown to a suitable size, isostatic leaves of the same size were selected. In the control group, 2 mL of the complex was injected into each treatment, and 60 $\mu$g of the plasmid was infiltrated into each leaf. After 24 h, the virus is inoculated by friction. Each treatment had three biological replicates at 25 °C and 16 h of light. The samples were collected at 2 and 4 dpi and frozen in liquid nitrogen.

Quantitative real-time reverse transcriptase PCR (qRT-PCR) was used for the relative expression assays. RNA was extracted using the Trizol reagent (Invitrogen) and stored at −80 °C for later use. The concentration of RNA was detected, and the cDNA was synthesized after the standard had been reached. All of the qRT-PCR reactions were performed in 10 $\mu$L reaction solutions with four technical replicates in a 96-well format and read using a 7500 Fast Realtime PCR system (Applied Biosystems) for the 96-well plates. With actin as an internal reference and the $C_t$ value of the control group as a standard value of 1, a qRT-PCR reaction was performed on ABI7500 using the relative method formula $2^{-\Delta\Delta C_t}$ to calculate the relative levels of expression of the virus in leaves that had been treated differently. qRT-PCR that incorporated SYBR Green qRT-PCR methodology was utilized. The data were analyzed with an independent sample *T*-test using IBM SPSS Statistics v.25 software. Differences were considered significant when $P < 0.05$.

**Western Blotting Assay.** The total protein from 100 mg of samples was extracted using a Pierce Classic IP Kit (Pierce), with protease inhibitors, lysis/wash buffer, halt protease (Thermo Scientific), and phosphatase inhibitor cocktails (Thermo Scientific). The proteins were separated on a 10% polyacrylamide gel. Immunoblot analysis was conducted using a rabbit antibody (1:5000, Invitrogen) for virus-expressed CP and virus CP antibody (1:2000) to detect the viral CP proteins. The antigens were detected by chemiluminescence using a reagent that detected an ECL reagent (SuperSignal West Pico Trial Kit). The intensity of bands was quantitatively measured using $\beta$-actin as an internal reference.

## DISCUSSION

Plant viral diseases are among the most serious pathogens in agricultural areas all over the world, and they deleteriously affect the development of crops.[16] Despite advances in genetic engineering in many biological species that can effectively prevent and cure viral diseases, the transport of biomolecules into plant cells remains one of the major limitations to the rapid, large-scale, and high-throughput implementation of plant genetic engineering, particularly intact plant tissues and organs.[17] Therefore, we proposed a gene delivery system using HACC as the gene carrier, which should be biocompatible, stable, and highly efficient.[18] The gene delivery system plays a key role in the delivery of antiviral genes in a broad spectrum of plants. This gene delivery system avoids the complicated experimental steps of *Agrobacterium* transformation and can highly efficiently deliver DNA to tobacco leaves without transgenic integration and with low toxicity and tissue damage.

While selecting nanodelivery materials, HACC is considered to be an effective gene delivery vector because it is positively charged and can easily combine with negatively charged plasmid DNA.[19] In this study, we report the successful preparation of the HACC/NbMLP28 complex and demonstrated its ability to be transiently expressed in cells. The size of the complex is crucial for cell uptake. The HACC/NbMLP28 complex prepared in this study is spherical, with sizes ranging


https://doi.org/10.1021/acsomega.1c05295
ACS Omega 2021, 6, 33953−33960

from 40 to 150 nm, and the plasmid is evenly distributed in the nanoparticle, which is an important feature of the cell delivery carrier.[20] Studies have shown that small complexes can enter the cells through endocytosis and pinocytosis,[21] thus improving the transfection efficiency of the delivery system. We prepared the complex gently, adjusted the concentration of HACC and plasmid, controlled the stirring rate and other parameters, and achieved control of the particle size and surface charge of the complex. The customization of these characteristics provided the best ratio and ideal efficacy. Another interesting result was that the final antiviral effect differed by changing the mass ratio of HACC to plasmid DNA (pDNA). Although the exact mechanism of HACC to pDNA mass ratio on the transfection efficiency is not clear, the most efficient antiviral effects took place when the mass ratio was 2:1. A correlation between the mass ratio of HACC to DNA and the transfection efficiency has also been reported in previous studies.[22] We hypothesize that the HACC/DNA complex protects pDNA from delivery barriers, such as intracellular proteins and DNA-degrading enzymes,[23] thereby improving the possibility of effective gene introduction into the nucleus and efficient gene expression. This method also facilitates the establishment of transient or stable gene expression systems to study plant−virus interactions at the cellular levels.[24]

While nanomaterials have been studied for gene delivery into animal cells,[25,26] their potential for plant systems merits more study. Most of the foundational studies deliver only nonfunctional cargoes, are conducted in protoplast cell culture, or use mechanical aids, such as gene guns[27] or ultrasound,[28] to enable the entry of nanoparticles into the walled plant cells. In addition, the global regulation of genetically modified organisms (GMOs) is driving the development of future approaches to nonintegrated or DNA-free plant genetic transformation, where the gene expression transmitted is transient, and foreign DNA is not integrated into the plant genome.[29] The commonly used plant transformation tool *Agrobacterium*-mediated transformation produces random gene integration, and the transgenic cycle is too long. Although the selection of resistant varieties is efficient and long-term, it still has the possibility of transgenic harm.[30] DNA transfer methods using gene guns or other external forces lead to cell damage,[31] which leads to an increase in the rate of transgenic integration.

Repair mechanisms in plants that result in stress DNA damage inevitably have an immeasurable impact on the quality and variety of crops. Therefore, the short-term gene delivery system presented in this paper, as a new method of the transient expression of the delivery of exogenous genes into plants, provides a new option for the development of antiviral resistance. Furthermore, HACC-based plant transient transformations are a useful addition to the plant biotechnology toolkit.

The world's staple food crops, and other food crops that optimize human nutrition, suffer from global virus disease pandemics and epidemics that greatly diminish their yields or produce quality.[32] We face significant challenges for food production, and an evaluation of actual practical applicability needs to be part of the entire research and development process if we are to develop viable and effective solutions.[33] Otherwise, we run the risk of wasting time on strategies that will never be useful in the real world. This nanodelivery system can improve the ability of plants to resist viruses economically and effectively and is conducive to the scale-up and economics production of crops.

## AUTHOR INFORMATION


### Corresponding Authors

**Songbai Zhang** − *Hubei Engineering Research Center for Pest Forewarning and Management, Yangtze University, Jingzhou 434025 Hubei, China*; Email: yangtze2008@126.com

**Jinguang Yang** − *Key Laboratory of Tobacco Pest Monitoring Controlling & Integrated Management, Tobacco Research Institute of Chinese Academy of Agricultural Sciences, Qingdao 266101, China*; orcid.org/0000-0002-9584-9634; Phone: +86-532-88703236; Email: yangjinguang@caas.cn

### Authors

**Daoshun Zhang** − *Hubei Engineering Research Center for Pest Forewarning and Management, College of Agriculture, Yangtze University, Jingzhou 434025 Hubei, China*; orcid.org/0000-0001-6053-4352

**Liyun Song** − *Key Laboratory of Tobacco Pest Monitoring Controlling & Integrated Management, Tobacco Research Institute of Chinese Academy of Agricultural Sciences, Qingdao 266101, China*

**Zhonglong Lin** − *China Tobacco Corporation Yunnan Company, Kunming 650001 Yunnan, China*

**Kun Huang** − *Honghe City Company of Yunnan Tobacco Company, Honghe 652399 Yunnan, China*

**Chunming Liu** − *Honghe City Company of Yunnan Tobacco Company, Honghe 652399 Yunnan, China*

**Yong Wang** − *Liangshan State Company of Sichuan Province Tobacco Company, Liangshan 615000 Sichuan, China*

**Dongyang Liu** − *Liangshan State Company of Sichuan Province Tobacco Company, Liangshan 615000 Sichuan, China*

Complete contact information is available at: https://pubs.acs.org/10.1021/acsomega.1c05295

### Author Contributions

#D.Z. and L.S. contributed equally to this work. All authors have given approval to the final version of the manuscript.


### Notes

The authors declare no competing financial interest.

## ACKNOWLEDGMENTS

This work was financially supported by Green Prevention and Control Program (110201901041(LS-04); 110202001033(LS-02)) and Science and Technology Project of China National Tobacco Corporation in Sichuan Province (SCYC202008).

## REFERENCES

(1) Pallás, V.; Sanchez-Navarro, J. A.; James, D. Recent Advances on the Multiplex Molecular Detection of Plant Viruses and Viroids. *Front. Microbiol.* **2018**, *9*, No. 2087.

(2) Jablonski, M.; Poghossian, A.; Keusgen, M.; Wege, C.; Schoning, M. J. Detection of plant virus particles with a capacitive field-effect sensor. *Anal. Bioanal. Chem.* **2021**, *413*, 5669−5678.

(3) Scholthof, K. B. G.; Adkins, S.; Czosnek, H.; Palukaitis, P.; Jacquot, E.; Hohn, T.; Hohn, B.; Saunders, K.; Candresse, T.; Ahlquist, P.; et al. Top 10 plant viruses in molecular plant pathology. *Mol. Plant Pathol.* **2011**, *12*, 938−954.

(4) Nessler, C. L.; Burnett, R. J. Organization of the major latex protein gene family in opium poppy. *Plant Mol. Biol.* **1992**, *20*, 749−752.
(5) Song, L.; Wang, J.; Jia, H.; Kamran, A.; Qin, Y.; Liu, Y.; Hao, K.; Han, F.; Zhang, C.; Li, B.; et al. Identification and functional characterization of NbMLP28, a novel MLP-like protein 28 enhancing Potato virus Y resistance in *Nicotiana benthamiana*. *BMC Microbiol.* **2020**, *20*, No. 55.
(6) Que, Q.; Chilton, M. M.; Elumalai, S.; Zhong, H.; Dong, S.; Shi, L. Repurposing Macromolecule Delivery Tools for Plant Genetic Modification in the Era of Precision Genome Engineering. In *Methods in Molecular Biology*; Humana Press, 2019; Vol. *1864*, pp 3−18.
(7) Nagpal, K.; Singh, S. K.; Mishra, D. N. Drug targeting to brain: a systematic approach to study the factors, parameters and approaches for prediction of permeability of drugs across BBB. *Expert Opin. Drug Delivery* **2013**, *10*, 927−955.
(8) Demirer, G. S.; Silva, T. N.; Jackson, C. T.; Thomas, J. B.; W, E. D.; Rhee, S. Y.; Mortimer, J. C.; Landry, M. P. Nanotechnology to advance CRISPR-Cas genetic engineering of plants. *Nat. Nanotechnol.* **2021**, *16*, 243−250.
(9) Dong, O. X.; Ronald, P. C. Targeted DNA insertion in plants. *Proc. Natl. Acad. Sci. U.S.A.* **2021**, *118*, No. e2004834117.
(10) Meng, W.; He, C.; Hao, Y.; Wang, L.; Li, L.; Zhu, G. Prospects and challenges of extracellular vesicle-based drug delivery system: considering cell source. *Drug Delivery* **2020**, *27*, 585−598.
(11) Almeida, A.; Gunday-Tureli, N.; Sarmento, B. A scale-up strategy for the synthesis of chitosan derivatives used in micellar nanomedicines. *Int. J. Pharm.* **2021**, *609*, No. 121151.
(12) Wang, F.; Zhang, Q.; Huang, K.; Li, J.; Wang, K.; Zhang, K.; Tang, X. Preparation and characterization of carboxymethyl cellulose containing quaternized chitosan for potential drug carrier. *Int. J. Biol. Macromol.* **2020**, *154*, 1392−1399.
(13) Li, Q.; Wang, W.; Hu, G.; Cui, X.; Sun, D.; Jin, Z.; Zhao, K. Evaluation of Chitosan Derivatives Modified Mesoporous Silica Nanoparticles as Delivery Carrier. *Molecules* **2021**, *26*, No. 2490.
(14) Lopez-Moya, F.; Escudero, N.; Zavala-Gonzalez, E. A.; Esteve-Bruna, D.; Blazquez, M. A.; Alabadi, D.; Lopez-Llorca, L. V. Induction of auxin biosynthesis and WOX5 repression mediate changes in root development in Arabidopsis exposed to chitosan. *Sci. Rep.* **2017**, *7*, No. 16813.
(15) Qin, Y.; Wang, J.; Wang, F.; Shen, L.; Zhou, H.; Sun, H.; Hao, K.; Song, L.; Zhou, Z.; Zhang, C.; et al. Purification and Characterization of a Secretory Alkaline Metalloprotease with Highly Potent Antiviral Activity from Serratia marcescens Strain S3. *J. Agric. Food Chem.* **2019**, *67*, 3168−3178.
(16) Jones, R. Global Plant Virus Disease Pandemics and Epidemics. *Plants* **2021**, *10*, No. 233.
(17) Demirer, G. S.; Zhang, H.; Matos, J. L.; Goh, N. S.; Cunningham, F. J.; Sung, Y.; Chang, R.; Aditham, A. J.; Chio, L.; Cho, M. J.; et al. High aspect ratio nanomaterials enable delivery of functional genetic material without DNA integration in mature plants. *Nat. Nanotechnol.* **2019**, *14*, 456−464.
(18) Liu, W.; Rudis, M. R.; Cheplick, M. H.; Millwood, R. J.; Yang, J. P.; Ondzighi-Assoume, C. A.; Montgomery, G. A.; Burris, K. P.; Mazarei, M.; Chesnut, J. D.; et al. Lipofection-mediated genome editing using DNA-free delivery of the Cas9/gRNA ribonucleoprotein into plant cells. *Plant Cell Rep.* **2020**, *39*, 245−257.
(19) Li, Q.; Wang, W.; Hu, G.; Cui, X.; Sun, D.; Jin, Z.; Zhao, K. Evaluation of Chitosan Derivatives Modified Mesoporous Silica Nanoparticles as Delivery Carrier. *Molecules* **2021**, *26*, No. 2490.
(20) Li, G. F.; Wang, J. C.; Feng, X. M.; Liu, Z. D.; Jiang, C. Y.; Yang, J. D. Preparation and testing of quaternized chitosan nanoparticles as gene delivery vehicles. *Appl. Biochem. Biotechnol.* **2015**, *175*, 3244−3257.
(21) Katas, H.; Alpar, H. O. Development and characterisation of chitosan nanoparticles for siRNA delivery. *J. Controlled Release* **2006**, *115*, 216−225.
(22) Nimesh, S.; Thibault, M. M.; Lavertu, M.; Buschmann, M. D. Enhanced gene delivery mediated by low molecular weight chitosan/DNA complexes: effect of pH and serum. *Mol. Biotechnol.* **2010**, *46*, 182−196.
(23) Bennett, M.; Deikman, J.; Hendrix, B.; Iandolino, A. Barriers to Efficient Foliar Uptake of dsRNA and Molecular Barriers to dsRNA Activity in Plant Cells. *Front. Plant Sci.* **2020**, *11*, No. 816.
(24) Acanda, Y.; Wang, C.; Levy, A. Gene Expression in Citrus Plant Cells Using Helios((R)) Gene Gun System for Particle Bombardment. In *Methods in Molecular Biology*; Humana Press, 2019; Vol. *2015*, pp 219−228.
(25) Song, S.; Hao, Y.; Yang, X.; Patra, P.; Chen, J. Using Gold Nanoparticles as Delivery Vehicles for Targeted Delivery of Chemotherapy Drug Fludarabine Phosphate to Treat Hematological Cancers. *J. Nanosci. Nanotechnol.* **2016**, *16*, 2582−2586.
(26) Mizrachi, A.; Shamay, Y.; Shah, J.; Brook, S.; Soong, J.; Rajasekhar, V. K.; Humm, J. L.; Healey, J. H.; Powell, S. N.; Baselga, J.; et al. Tumour-specific PI3K inhibition via nanoparticle-targeted delivery in head and neck squamous cell carcinoma. *Nat. Commun.* **2017**, *8*, No. 14292.
(27) Martin-Ortigosa, S.; Valenstein, J. S.; Sun, W.; Moeller, L.; Fang, N.; Trewyn, B. G.; Lin, V. S.; Wang, K. Parameters affecting the efficient delivery of mesoporous silica nanoparticle materials and gold nanorods into plant tissues by the biolistic method. *Small* **2012**, *8*, 413−422.
(28) Liu, J.; Wang, F.; Wang, L.; Xiao, S.; Tong, C.; Tang, D.; Liu, X. Preparation of fluorescence starch-nanoparticle and its application as plant transgenic vehicle. *J. Cent. South Univ. Technol.* **2008**, 768−773.
(29) Cunningham, F. J.; Goh, N. S.; Demirer, G. S.; Matos, J. L.; Landry, M. P. Nanoparticle-Mediated Delivery towards Advancing Plant Genetic Engineering. *Trends Biotechnol.* **2018**, *36*, 882−897.
(30) Li, Y.; Wang, K.; Lu, Q.; Du, J.; Wang, Z.; Wang, D.; Sun, B.; Li, H. Transgenic *Nicotiana benthamiana* plants expressing a hairpin RNAi construct of a nematode Rs-cps gene exhibit enhanced resistance to Radopholus similis. *Sci. Rep.* **2017**, *7*, No. 13126.
(31) Lv, Z.; Jiang, R.; Chen, J.; Chen, W. Nanoparticle-mediated gene transformation strategies for plant genetic engineering. *Plant J.* **2020**, *104*, 880−891.
(32) Jones, R. Global Plant Virus Disease Pandemics and Epidemics. *Plants* **2021**, *10*, No. 233.
(33) Zhu, X.; Yuan, X.; Zhang, Y.; Liu, H.; Wang, J.; Sun, B. The global concern of food security during the COVID-19 pandemic: Impacts and perspectives on food security. *Food Chem.* **2022**, *370*, No. 130830.


https://doi.org/10.1021/acsomega.1c05295
*ACS Omega* 2021, 6, 33953−33960